A Novel Zeolite-Induced Population of a Planar Viologen Conformation. New Viologen Charge Transfer Complexes and Alkene/Viologen/Zeolite Arrays

Andrea Pace,[†] Edward L. Clennan,*[,‡] Frank Jensen,[§] and Jamie Singleton[‡]

Department of Chemistry, University of Wyoming, Laramie, Wyoming 82071, Dipartimento di Chimica Organica "E. Paternò", Università degli Studi di Palermo, Viale delle Scienze, Parco d'Orleans II, 90128, Palermo, Italy, and Department of Chemistry, Odense University, DK-5230 Odense M., Denmark

Received: July 28, 2003; In Final Form: February 10, 2004

A rare example of a novel zeolite-induced conformational change and a mechanism for this process are suggested in order to rationalize an unexpected spontaneous intrazeolite reduction observed during preparation of a new viologen (MQ^{2+})-doped zeolite (NaY). In addition, the formations of six new alkene/viologen/zeolite charge transfer (CT) arrays using NaMQY and the previously reported NaMVY are also reported. The binding constants between MQ^{2+} and MV^{2+} and 2,3-dimethyl-2-butene (TME) were determined using the Benesi−Hildebrand approach, and the stabilities of these CT complexes are compared to their intrazeolite analogue.

Introduction

Viologens (Chart 1) have been extensively utilized as electron acceptors in molecular assemblies designed to store solar energy, as herbicides to inhibit reduction of ferredoxin in photosystem I, and as components of electrochromic display devices.[1] As a result, their chemistry in solution has been extensively examined. In particular, their electrochemical behavior and their ability to form both intra- and intermolecular charge transfer (CT) complexes with a wide range of donors including halides,[2,3] ferrocyanide,[4] carboxylate anions,[5] amines,[6] phenols, and arenes[7] have been documented. Kochi and Yoon[8] have taken advantage of this propensity to form CT complexes and have used viologens to detect incorporation and diffusion of arenes in zeolites. Park and co-workers[9] pointed out that these CT complexes are more properly viewed as (arene/viologen/zeolite) arrays because simultaneous viologen/arene and viologen/zeolite CT interactions can be spectroscopically observed.

Zeolites are crystalline solids consisting of catenated silicon and aluminum tetrahedra that enclose regular repeating cavities or channels of well-defined size and shape.[10] The zeolite NaY (Chart 2) is characterized by a large spherical supercage 13 Å in diameter accessible via four tetrahedrally arranged 7.4 Å windows. Exchangeable sodium cations are associated with each of the negatively charged tetrahedral aluminum atoms in the eight supercages comprising a unit cell.

The ability of zeolites to dramatically influence product distribution in both chemical and photochemical reactions has been amply documented. Changes in the conformations of the absorbed molecules[11,12] certainly play an important role in this ability of zeolites to influence product distribution. However, in situ conformational analysis is uncommon[13−16] and a direct relationship between conformation and reactivity has rarely been documented.[17] A noteworthy exception to this generalization is the work of Calzaferri and co-workers[18] who used an impressive array of analytical techniques and computational tools to establish that methyl viologen, MV^{2+}, is twisted about the single bond connecting the two pyridyl rings when embedded in zeolite L. As part of our ongoing effort to generate new oxygenation catalysts[19] we report here synthesis of new alkene/viologen/zeolite arrays and a spontaneous intrazeolite reduction of a viologen which we tentatively attribute to a conformational change induced by absorption in a very constrained location in the zeolite.

CHART 1

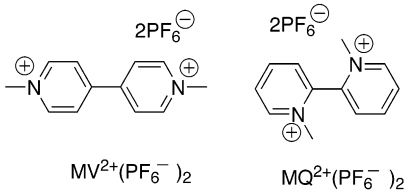

CHART 2

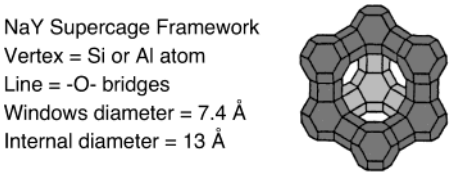

Results and Discussion

Synthesis of Viologen-Doped Zeolites. Viologens MV^{2+} and MQ^{2+} (Chart 1) were loaded into NaY by ion exchange from aqueous solutions to obtain loading levels of <viologen> = 1.0 (average number of molecules per supercage) as reported previously for MV^{2+}.[20] Incorporation of ion pairs, $MVCl^+$, during exchange with $MVCl_2$ although possible, can be ruled out based upon substantial literature precedent.[20−22] In addition, X-ray photoelectron spectroscopy (XPS) has ruled out ion pair ($MVCl^+$) incorporation even in zeolites NaZSM-5 and Al-

* Author to whom correspondence should be addressed. E-mail: Clennane@uwyo.edu.
[†] Università degli Studi di Palermo.
[‡] University of Wyoming.
[§] Odense University.

10.1021/jp036200p CCC: $27.50
Published on Web 03/19/2004

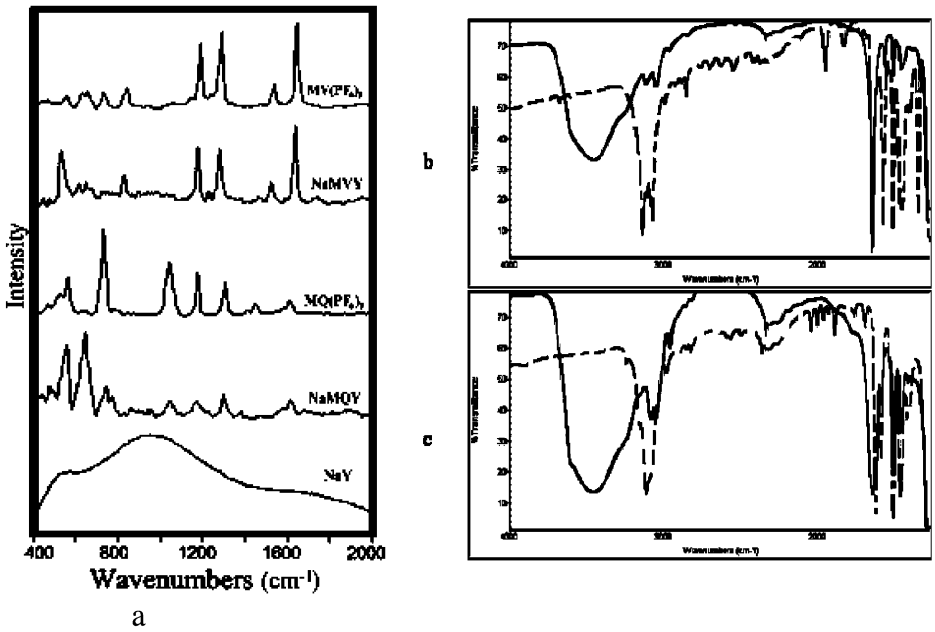

Figure 1. (a) Raman spectra of viologen hexafluorophosphate salts and viologen-doped NaY. (b) IR spectra (4000−1270 cm^{-1}) recorded in Fluorolube of NaMVY (—) and $MV(PF_6)_2$ (- - -). (c) IR spectra (4000−1270 cm^{-1}) recorded in Fluorolube of NaMQY (—) and $MQ(PF_6)_2$ (- - -).

MCM-41 where monopositive ion pair incorporation would be considered more likely because of the greater distance between the charge-balancing aluminum framework sites.[23] Nevertheless, because MQ^{2+} had not been previously incorporated into NaY, we took the added precaution to first convert MQI_2 to the hexafluorophosphate salt[24] which is less likely to form a $MQPF_6^+$ ion pair and has enough solubility at 60 °C in water to allow zeolite incorporation by ion exchange. The loading level was determined by monitoring the concentration of viologen remaining in solution after ion exchange by UV spectroscopy. In order to distinguish between supercage-incorporated viologen and viologen physically absorbed on the external surface of the zeolite, a colorimetric test was employed. This test involved addition of the viologen-doped zeolite to a saturated KI/acetonitrile solution. The development of a yellow-colored solution and yellow zeolite powder is indicative of both incorporated and physically absorbed viologen. The zeolite samples were washed with water until under the test conditions the powder but not the acetonitrile solution turned yellow. The combined washings were then analyzed by UV in order to calculate the final loading levels of the doped zeolites. The washed samples of the viologen-doped zeolites were then dried for at least 24 h at 100 °C (NaMVY) or 40 °C (NaMQY) and 10^{-4} Torr.

Methyl viologen, MV^{2+}, is known to decompose in NaMor (sodium mordenite) by a demethylation route at high temperatures.[23] For this reason, the structural integrity of the embedded viologens was demonstrated by diffuse reflectance UV−vis spectroscopy, FT-IR, Raman spectroscopy (Figure 1),[25] and ^{13}C high-resolution CPMAS NMR (see the Supporting Information).

Samples of NaMQ⟨1.0⟩Y (⟨1.0⟩ refers to the loading level in molecules per supercage of the *preceding* component in the zeolite array) heated at 100 °C and 10^{-4} Torr developed a light-blue coloration (diffuse reflectance UV−vis spectroscopy revealed a new broad band at $\lambda_{MAX} = 628$ nm; see the Supporting Information) reminiscent of the blue color of the nearly planar[26] methyl viologen radical cation ($MV^{\bullet+}$). Consistent with the assignment of this species to a near planar $MQ^{\bullet+}$ are RPA/6-31G(d) excitation energies of 620 and 692 nm calculated for $MQ^{\bullet+}$ held at NCCN dihedral angles of 10° and 170 °C, respectively. Also consistent with this interpretation is the observation of a very weak intrazeolite ESR signal (see the Supporting Information) that disappeared together with the blue color upon exposure of the sample to air, with a g value of 2.0027 ± 0.0003 similar to the g value of 2.0030[27] reported for $MV^{\bullet+}$. However, in dramatic contrast to $MV^{\bullet+}$, the radical cation $MQ^{\bullet+}$ B3LYP/6-31G(d) rotational energy profile (Figure 2a) exhibits minima far from a planar geometry at approximately 45° and 135°. The RPA/6-31G(d) excitation energies at these energy minima are approximately 985 nm, inconsistent with the blue coloration. Consequently, it is tempting to suggest that a very small amount of planar radical cation is formed in a very constrained location in the zeolite cavity.

Electrochemical attempts to independently generate stable solutions of $MQ^{\bullet+}$ failed. Braterman and Song[28] also noted the instability of $MQ^{\bullet+}$ and attributed it to a combination of steric and electronic effects. Cyclic voltammetry studies confirmed the reactivity of $MQ^{\bullet+}$ and demonstrated the very dramatic difference in the stabilities of $MV^{\bullet+}$ and $MQ^{\bullet+}$ (see the Supporting Information). However, reduction of $NaMQ^{2+}Y$ with solvated electrons (K/18-crown-6)[11] produced a brown solid which exhibited a broad diffuse reflectance UV−vis band with a maximum at approximately 950 nm and a single line ESR spectrum ($g = 2.0036 \pm 0.0009$) (see the Supporting Information). Both the ESR signal and the broad UV−vis band disappeared upon exposure to oxygen. This provides dramatic confirmation of the RPA/6-31G(d) calculations and a remarkable example of kinetic stabilization of a reactive species ($MQ^{\bullet+}$) by the inorganic host.

The molecular mechanics (MMX) rotational energy profile (Figure 2b) demonstrates that MQ^{2+} is similar to $MQ^{\bullet+}$ and also prefers a twisted nonplanar geometry. Consequently, one can envision two limiting mechanisms as shown in Scheme 1 for the formation of the planar radical cation. In the first mechanism both a twisted and planar $MQ^{\bullet+}$ are formed by electron donation from the zeolite framework. In the second mechanism a twisted $MQ^{\bullet+}$ is never formed; instead a small amount of planar MQ^{2+} is selectively reduced to form the radical cation. Mechanism I can be ruled out because no near-infrared peak at 985 nm as predicted by the RPA/6-31G(d) calculations

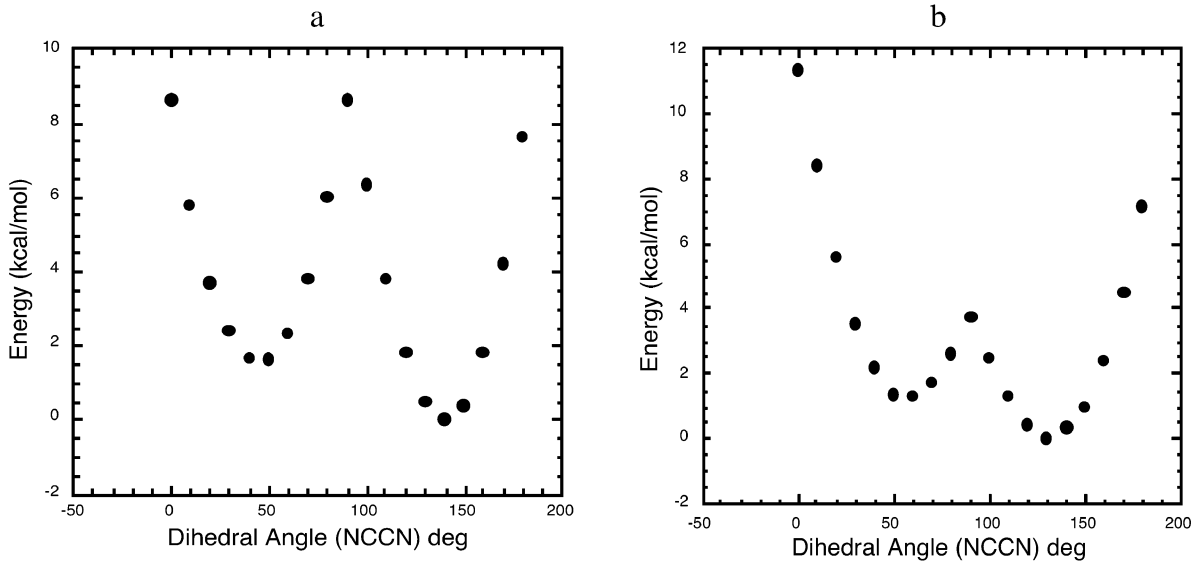

Figure 2. Rotational energy profiles of (a) $MQ^{\bullet+}$ calculated with B3LYP/6-31G(d) optimized geometries and (b) MQ^{2+} calculated with the force field MMX.

SCHEME 1: Two Limiting Mechanisms for the Formation of Planar MQ Radical Cation

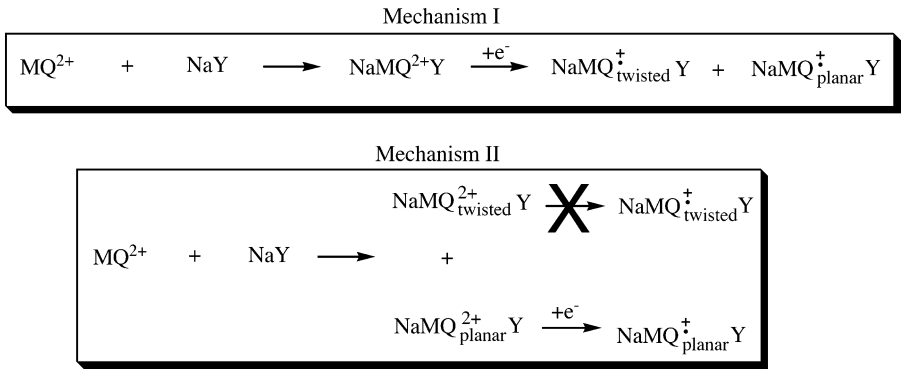

or at 950 nm as demonstrated experimentally (vide supra) for the twisted radical cation was observed. Instead we suggest that a very small amount of planar MQ^{2+} is formed in a very constrained zeolite environment. Previous observations[29,30] of linear relationships between reduction potentials and calculated viologen NCCN dihedral angles suggest that this planar conformation is more easily reduced than the twisted conformation, and as a result selective formation of the planar radical cation is observed. Unfortunately, the very small amount of planar radical cation formed (we estimate $\ll$1 $MQ^{\bullet+}$ per unit cell) precludes a definitive discussion of the identity of the electron donor or of the location and/or nature of the constrained sites. We note, however, the distinct possibility that defect sites and/or impurities (e.g., Fe) could be involved in this unusual observation.[31]

Synthesis of Intrazeolite CT Complexes. Zeolite array NaMV⟨1.0⟩TME⟨1.0⟩Y was generated by addition of neat 2,3-dimethyl-2-butene (TME) to a powdered sample of NaMV-⟨1.0⟩Y. The addition was accompanied by the instantaneous development of a distinctive yellow color. Examination of the sample by diffuse reflectance UV−vis spectroscopy revealed formation of a new broad band at $\lambda_{MAX} = 375$ nm (Figure 3a). Similar doping with cyclohexene (CH) and 2-methyl-2-butene (2M2B) also produced light to very light yellow-colored zeolite arrays. A comparison of the diffuse reflectance UV−vis spectra of the three alkene/viologen/zeolite arrays (Figure 3b) reveals that the CH and 2M2B arrays are characterized by shoulders on the intense NaMVY absorption rather than by distinct peaks.

The assignment of the 375 nm band to an intrazeolite charge transfer complex between MV^{2+} and TME is compatible with a Mulliken analysis.[32−34] In particular, the TME point falls remarkably close to a correlation line of absorption maximum, ν_{CT}, versus ionization potential, IP, previously established for a series of intrazeolite MV^{2+}/arene charge transfer complexes[20] (Figure 4a). The hypsochromic shift of the observed absorption profile (Figure 3b) in the zeolite array series containing TME, 2M2B, and CH is also in accord with the change in ionization potentials of the alkenes (TME = 8.27 eV;[35] 2M2B = 8.68 eV;[35] CH = 9.24 eV[36]) and predicted λ_{MAX} values (TME = 358 nm; 2M2B = 318 nm; CH = 276 nm) from Figure 4a. In addition, Benesi−Hildebrand[37] analysis (Figure 4b) of the MV^{2+}/TME charge transfer complex observed in CH_3CN gives an equilibrium constant for formation, $K_{eq} = 0.50 \pm 0.06$, which, as expected, is of the same order of magnitude as those observed for arenes[38] (e.g., MV^{2+}/naphthalene = 0.7; MV^{2+}/pentamethylbenzene = 0.8).

MQ^{2+} also exhibits easily detected TME, 2M2B, and CH CT arrays (Figure 5). Their hypsochromic shifts relative to their MV^{2+} analogue reveal their decreased stability. This decrease in stability was anticipated based upon two factors: (1) MQ^{2+} ($E° = -0.76$ V vs SCE) is more than 7 kcal/mol more difficult to reduce than MV^{2+} ($E° = -0.45$ V vs SCE) and (2) the viologen nucleus in MV^{2+} CT complexes prefers a radical cation-like near planar conformation rather than a dication-like more twisted conformation.[8] However, both MQ^{2+} and $MQ^{\bullet+}$ (in contrast to $MV^{\bullet+}$) are significantly twisted (vide supra) and

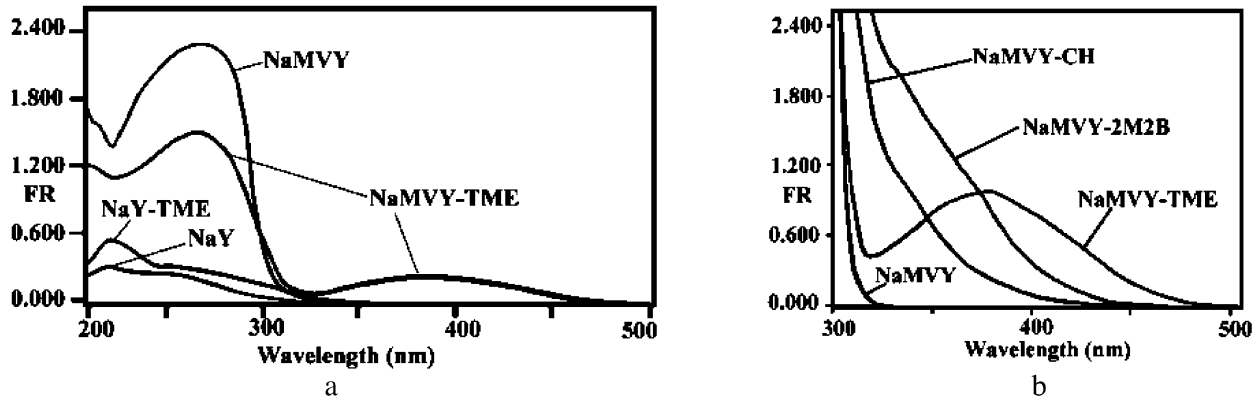

Figure 3. (a) Diffuse reflectance UV−vis spectra of NaMV⟨1.0⟩ TME⟨1.0⟩Y compared to undoped, and TME- and MV-doped samples all diluted in an alumina matrix. (b) Comparison of the diffuse reflectance UV−vis spectra of methyl viologen zeolite arrays undoped (NaMVY) and doped (⟨s⟩ = 1.0) with 2,3-dimethyl-2-butene (TME), cyclohexene (CH), and 2-methyl-2-butene (2M2B).

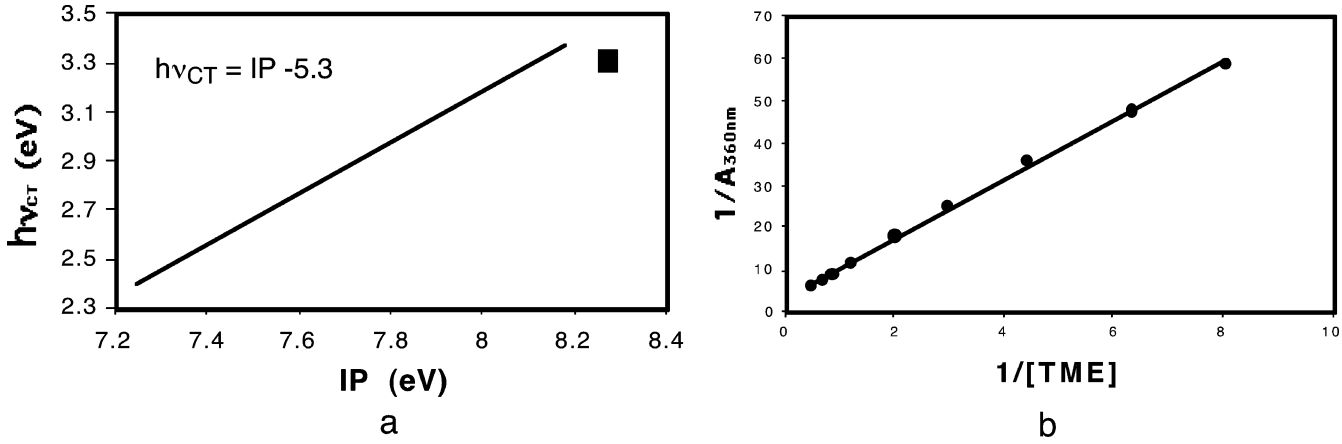

Figure 4. (a) Point (■) for charge transfer maximum NaMV⟨1.0⟩ TME⟨1.0⟩Y superimposed upon the Mulliken plot reported in ref 20. (b) Benesi−Hildebrand plot for MV^{2+}/TME CT complex formation in acetonitrile monitored at 360 nm.

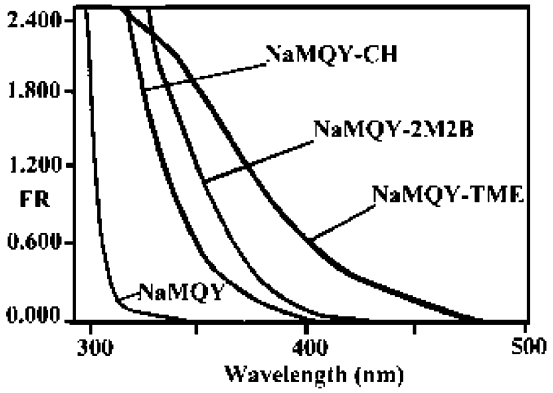

Figure 5. Comparison of the diffuse reflectance UV−vis spectra of alkene/viologen/zeolite CT arrays to that of NaMQY.

presumably cannot adopt for steric reasons an electronically more favorable near planar geometry for the formation of the CT complex. The decreased stability of the MQ^{2+}/TME CT complex is also evident in solution. Benesi−Hildebrand treatment of MQ^{2+}/TME in acetonitrile gives a $K_{eq} = 0.25 \pm 0.04$ that is only 50% of the magnitude of the K_{eq} measured for the MV^{2+}/TME complex (vide supra).

The onset of the CT bands in the doped zeolites were bathochromically shifted by 65 nm (440 nm → 505 nm) for MV^{2+}/TME and by 90 nm for MQ^{2+}/TME (390 nm → 480 nm) from their corresponding values in acetonitrile (see the Supporting Information). These shifts reflect a greater than 8 and 13 kcal/mol stabilization, respectively, of the MV^{2+} and MQ^{2+} CT complexes by the electrostatic field and the confined environment in the interior of the NaY. These stabilization energies are much smaller than the 70−80 kcal/mol values reported for alkene/oxygen CT complexes.[39] These smaller stabilization energies probably reflect the charge shift (acceptor^{2+}/alkene → acceptor$^{\bullet+}$/alkene$^{\bullet+}$) character of the viologen CT complexes and the resulting smaller changes in the dipole moments rather than the charge formation (acceptor/alkene → acceptor$^{\bullet-}$/alkene$^{\bullet+}$) character observed for alkene/oxygen CT complexes.

MQ^{2+} CT complexes are more influenced by environmental changes than their MV^{2+} analogues as revealed by the observed hypsochromic shifts of their absorption onsets (5 nm for MV^{2+}/TME and 20 nm for MQ^{2+}/TME) in moving the complex from NaY to CsY (see the table in the Supporting Information). These counterion-induced shifts, which have also been reported for MV^{2+}/arene complexes in different MY zeolites,[21] are due to the dual influence of the size of Cs^+ and its ability to impart higher donor properties to the zeolite framework.

Conclusion

A new viologen-doped zeolite NaMQ⟨1.0⟩Y has been reported, and its spontaneous partial reduction to a radical cation has been observed. This spontaneous reduction has been tentatively attributed to a very unusual zeolite-enforced change from the twisted solution energy minimum geometry of MQ^{2+} to a more easily reduced planar conformation. In addition, several new alkene/viologen/zeolite arrays have been generated and characterized. These zeolite-based materials provide new

opportunities to determine if the internal energy in viologen$^{\bullet+}$/alkene$^{\bullet+}$ ion pairs generated by photochemical activation can be harnessed to do useful chemical work. Zeolites provide a unique medium for these types of applications because of their well-established ability to inhibit energy-wasting back electron transfer.[40]

Experimental Section

Preparation of $MQ(PF_6)_2$ and $MV(PF_6)_2$. MQI_2 was prepared as reported[24] by mixing 5 g of 2,2′-bipyridine (from TCI), 15 mL of ethanol (95%), and 10 mL of CH_3I in a sealed tube. This mixture was then heated in an oil bath at 90−100 °C for 3 days. Solvent removal allowed the isolation of MQI_2. Addition of a concentrated aqueous solution of NH_4PF_6 to an aqueous solution of MQI_2 is followed by formation of a white precipitate of $MQ(PF_6)_2$ that was recrystallized three times from *n*-propanol/acetonitrile (3:1). $MV(PF_6)_2$ was prepared by a similar ion exchange procedure starting from the commercially available $MVCl_2$ salt (from Aldrich).[20]

Loading of Viologen in NaY. NaY (from Aldrich lot no. JI20903EI) was treated with a 1 M aqueous NaCl solution to ensure the elimination of other cation and Brønsted acid sites inside the supercage. Methyl viologen (MV^{2+}) was loaded into the zeolite as previously reported[20] by suspending 7.8 g of NaY (0.0036 N_A of supercages) in 500 mL of an aqueous solution of $MVCl_2$ monohydrate (1 g; 3.6 mmols) and by stirring the suspension overnight. The NaMVY was then filtered and washed several times until a negative Ag^+ test for chloride in the washing solution was obtained. The concentrations of MV^{2+} in the wash solutions were checked by measuring the UV absorption at 257 nm. This test revealed incorporation of all but 1% of the initial MV^{2+} thus indicating a loading level of $\langle MV \rangle = 1.0$. Similarly MQ^{2+} was loaded into the zeolite by suspending 9.1 g of NaY (0.0042 N_A of supercages) in an aqueous solution of $MQ(PF_6)_2$ (2 g; 4.2 mmols) kept at 60 °C and stirring the suspension overnight. NaMQY was filtered and washed several times until no trace of MQ^{2+} was detected at 267 nm in the wash solutions. Less than 1% of MQ^{2+} was unsuccessfully incorporated in the zeolite to give a loading level of $\langle MQ \rangle = 1.0$. A colorimetric test with saturated KI in acetonitrile was performed on small samples of both NaMQY and NaMVY to assess if any of the viologen dication was physically absorbed outside the cage instead of being ion exchanged with the cation into the supercage. The development of a yellow-colored zeolite powder and a colorless solution indicates exclusive incorporation of the viologen inside the supercage and its absence on the outer surface. NaMQY and NaMVY were dried prior to use for at least 24 h on a vacuum line at 10^{-4} Torr and at 40 °C and 100 °C, respectively.

Loading of Alkene in Viologen-Doped Zeolite. 2,3-Dimethyl-2-butene (16.8 mg; 0.2 mmols), 2-methyl-2-butene (14 mg; 0.2 mmols), or cyclohexene (16.4 mg) were added as neat liquids to 0.356 g (0.0002 N_A of supercages) of either NaMVY or NaMQY and allowed to equilibrate at room temperature for at least 1 h to obtain the corresponding alkene⟨1.0⟩/viologen-⟨1.0⟩/zeolite array.

Reduction of NaMQ⟨1.0⟩Y with Solvated Electrons. 400 mg of NaMQ⟨1.0⟩Y was added in a nitrogen-purged glovebox to 5 mL of a THF solution of solvated electrons prepared as reported previously[11] using 1 equiv of potassium metal and 18-crown-6. This sample was allowed to stir for 6 h. The brown solid was then filtered and loaded into an ESR tube and a diffuse reflectance cell for collection of spectral data. Both samples were sealed to prevent exposure to air.

Benesi−Hildebrand Treatment of TME/Viologen CT Complexes. $MV(PF_6)_2$ (29.5 mg) was dissolved in acetonitrile in a 10 mL volumetric flask to give a 0.0062 M solution of MV^{2+}. A 2.5 mL sample of this solution was placed into a quartz UV cuvette and the absorbance values (A_{MV}) were measured in 10 nm steps from 330 to 420 nm. A series of TME aliquots were then added to this solution, the UV spectra taken after each addition, and the absorbance values ($A_{MV/TME}$) recorded in 10 nm steps. These values were then corrected by contributions from MV^{2+} (A_{MV}) and/or TME (A_{TME}) as determined in separate experiments at the measured wavelengths as shown in eq 1.

$$A_{corrected}(\lambda) = A_{MV/TME}(\lambda) - A_{MV}(\lambda) - A_{TME}(\lambda) \quad (1)$$

The use of the Benesi−Hildebrand (BH) approach to determine equilibrium constants for very weak ($K_{eq} < 0.1$) and weak ($0.2 < K_{eq} < 1$) CT complexes has been extensively discussed.[41−43] Inherent limitations pointed out by Hammond[44] suggest the use of the form of the BH equation given in eq 2 for complexes with $0.2 < K_{eq} < 1$ in which $\epsilon(\lambda)$ is the molar extinction coefficient at the wavelength λ, $[MV^{2+}]_{initial} = 0.0062$, $[TME]_{added}$ is the total concentration of TME, and K_{eq} is the binding constant between TME and MV^{2+}. A plot of eq 2 from data recorded at 360 nm for MV^{2+}/TME (Figure 4b) gave a straight line ($R = 0.998$) whose slope and intercept were used to determine $K_{eq} = 0.50 \pm 0.06$ and ϵ (360 nm) $= 46 \pm 6$. The K_{eq} and ϵ values are both greater than 3 times their respective standard deviations validating the use of this approach.[41−44] The same values, within experimental error, were also obtained by using data recorded at 370 and 380 nm. Analysis of data recorded at longer wavelengths suffers from errors associated with the determination of very small absorbance values, whereas analysis of data recorded at shorter wavelengths suffers from the increasing influence of the MV^{2+} absorbance. The use of similar methodology for the study of the CT complex between MQ^{2+} and TME data recorded at 320 nm gave a straight line ($R = 0.997$) from which a $K_{eq} = 0.25 \pm 0.04$ and an ϵ (320 nm) $= 90 \pm 10$ were determined.

$$\frac{1}{A_{corrected}(\lambda)} = \frac{1}{K_{eq}\epsilon(\lambda)[MV^{2+}]_{initial}} \frac{1}{[TME]_{added}} + \frac{1}{\epsilon(\lambda)[MV^{2+}]_{initial}} \quad (2)$$

Computational Studies. Geometry optimizations were performed with the Gaussian 98 program package[45] at the B3LYP level with the 6-31G(d) basis set.[46] RPA calculations[46] were performed with the DALTON[47] program package. The molecular mechanics calculations were done with the MMX force field found in PCMODEL 7.0.[48]

Acknowledgment. We thank the National Science Foundation and the Italian CNR for their generous support of this research. We also thank Professors Jeff Yarger, Keith Carron, and Dan Buttry for assistance in the solid state NMR, Raman spectroscopy, and electrochemical experiments, respectively.

Supporting Information Available: IR spectra and data and Raman data for NaMV⟨1.0⟩Y, $MQ(PF_6)_2$, and NaMQ⟨1.0⟩Y; table of UV−vis onset values for viologens CT complexes in NaY and CsY; ESR and diffuse reflectance UV−vis spectra of light blue NaMQ⟨1.0⟩Y; ESR and diffuse reflectance UV−vis spectra of the product from reduction of NaMQ⟨1.0⟩Y with

solvated electrons; ^{13}C high-resolution CPMAS NMR for NaMV⟨1.0⟩Y and NaMQ⟨1.0⟩Y; Benesi−Hildebrand plot for MQ^{2+}/TME in acetonitrile; cyclic voltammograms for MV^{2+} and MQ^{2+}. This material is available free of charge via the Internet at http://pubs.acs.org.

References and Notes

(1) Monk, P. M. S. *The Viologens. Physicochemical Properties, Synthesis and Applications of the Salts of 4, 4′-Bipyridine*; John Wiley & Sons: Chichester, U.K., 1998.

(2) Bertolotti, S. G.; Cosa, J. J.; Gsponer, H. E.; Previtali, C. M. *Can. J. Chem.* **1983**, *65*, 2425−2427.

(3) Monk, P. M. S.; Hodgkinson, N. M. *Electrochim. Acta* **1998**, *43*, 245−255.

(4) Hammach, W. C.; Drickamer, H. G.; Hendrickson, D. N. *Chem. Phys. Lett.* **1988**, *151*, 469−473.

(5) Bockman, T. M.; Hubig, S. M.; Kochi, J. K. *J. Org. Chem.* **1997**, *62*, 2210−2221.

(6) Byrd, H.; Suponeva, E. P.; Bocarsly, A. B.; Thompson, M. E. *Nature* **1996**, *380*, 610−612.

(7) Hubig, S. M.; Kochi, J. K. *J. Phys. Chem.* **1995**, *99*, 17587−17585.

(8) Yoon, K. B.; Kochi, J. K. *J. Am. Chem. Soc.* **1989**, *111*, 1128−1130.

(9) Park, Y. S.; Um, S. Y.; Yoon, K. B. *J. Am. Chem. Soc.* **1999**, *121*, 3193−3200.

(10) Dyer, A. *An Introduction to Zeolite Molecular Sieves*; John Wiley & Sons: New York, 1988.

(11) Park, Y. S.; Lee, K.; Lee, C.; Yoon, K. B. *Langmuir* **2000**, *16*, 4470−4477.

(12) Brémard, C.; Buntinx, G.; Coustillier, G.; Ginestet, G. *J. Mol. Struct.* **1997**, *410*−*411*, 81−84.

(13) Crawford, M. K.; Dobbs, K. D.; Smalley, R. J.; Corbin, D. R.; Maliszewskyj, N.; Udovic, T. J.; Cavanagh, R. R.; Rush, J. J.; Grey, C. P. *J. Phys. Chem. B* **1999**, *103*, 431−434.

(14) Huang, Y. *J. Phys. Chem. B* **2003**, *107*, 7647−7653.

(15) Huang, Y.; Leech, J. H.; Wang, H. *J. Phys. Chem. B* **2003**, *107*, 7632−7639.

(16) Roland, J.; Michel, D.; Pampel, A. In *Magnetic Resonance in Colloid and Interface Science*; Fraissard, J., Lapina, O., Eds.; Kluwer Academic Publishers: Dordrecht, The Netherlands, 2002; Vol. 76, pp 83−95.

(17) Serralha, F. N.; Lopes, J. M.; Ferreira, L. F. V.; Lemos, F.; Prazeres, D. M. F.; Aires-Barros, M. R.; Cabral, J. M. S.; Ribeiro, F. R. *Catal. Lett.* **2001**, *73*, 63−66.

(18) Hennessy, B.; Megelski, S.; Marcolli, C.; Shklover, V.; Bärlocher, C.; Calzaferri, G. *J. Phys. Chem. B* **1999**, *103*, 3340−3351.

(19) Clennan, E. L.; Sram, J. P. *Tetrahedron* **2000**, *56*, 6945−6950.

(20) Yoon, K. B.; Kochi, J. K. *J. Phys. Chem.* **1991**, *95*, 3780−3790.

(21) Alvaro, M.; García, H.; García, S.; Fernández, L. *Tetrahedron Lett.* **1996**, *37*, 2873−2876.

(22) Alvaro, M.; Ferrer, B.; Fornés, V.; García, H.; Scaiano, J. C. *J. Phys. Chem. B* **2002**, *106*, 6815−6820.

(23) Alvaro, M.; García, H.; García, S.; Márquez, F.; Scaiano, J. C. *J. Phys. Chem. B* **1997**, *101*, 3043−3051.

(24) Elliott, C. M.; Hershenhart, E. J. *J. Am. Chem. Soc.* **1982**, *104*, 7519−7526.

(25) Raman spectra were acquired on an Advantage 200A (DeltaNu, Laramie, WY).

(26) Mizuguchi, J.; Karfunkel, H. *Ber. Bunsen-Ges. Phys. Chem.* **1993**, *97*, 1466−1472.

(27) Rieger, A. L.; Rieger, P. H. *J. Phys. Chem.* **1984**, *88*, 5845−5851.

(28) Braterman, P. S.; Song, J.-I. *J. Org. Chem.* **1991**, *56*, 4678−4682.

(29) Willner, I.; Ayalon, A.; Rabinovitz, M. *New. J. Chem.* **1990**, *14*, 685−688.

(30) Wang, Y.; Zhao, W. *Molecules* **2000**, *5*, 1379−1385.

(31) García, H.; Roth, H. D. *Chem. Rev.* **2002**, *102*, 3947−4008.

(32) Mulliken, R. S. *J. Am. Chem. Soc.* **1952**, *74*, 811−824.

(33) Foster, R. *Organic Charge-Transfer Complexes*; Academic Press: New York, 1969; Vol. 15.

(34) Bender, C. J. *Chem. Soc. Rev.* **1986**, *15*, 475−502.

(35) Nelson, D. J.; Li, R.; Brammer, C. *J. Org. Chem.* **2001**, *66*, 2422−2428.

(36) Collin, J.; Lossing, F. P. *J. Am. Chem. Soc.* **1959**, *81*, 2064−2066.

(37) Benesi, H. A.; Hildebrand, J. H. *J. Am. Chem. Soc.* **1949**, *71*, 2703−2707.

(38) Yoon, K. B. In *Solid State and Surface Photochemistry*; Ramamurthy, V., Schanze, K. S., Eds.; Marcel Dekker Inc.: New York, 2000; Vol. 5, pp 143−251.

(39) Blatter, F.; Frei, H. *J. Am. Chem. Soc.* **1993**, *115*, 7501−7502.

(40) Yoon, K. B.; Hubig, S. M.; Kochi, J. K. *J. Phys. Chem.* **1994**, *98*, 3865−3871.

(41) Hoenigman, S. M.; Evans, C. E. *Anal. Chem.* **1996**, *68*, 3274−3276.

(42) Kuntz, I. D., Jr.; Gasparro, F. P.; Johnston, M. D., Jr.; Taylor, R. P. *J. Am. Chem. Soc.* **1968**, *90*, 4778−4781.

(43) Zaini, R.; Orcutt, A. C.; Arnold, B. R. *Photochem. Photobiol.* **1999**, *69*, 443−447.

(44) Hammond, P. R. *J. Chem. Soc.* **1964**, 479−484.

(45) Frisch, M. J.; Trucks, G. W.; Schlegel, H. B.; Scuseria, G. E.; Robb, M. A.; Cheeseman, J. R.; Zakrzewski, V. G.; Montgomery, J. A., Jr.; Stratmann, R. E.; Burant, J. C.; Dapprich, S.; Millam, J. M.; Daniels, A. D.; Kudin, K. N.; Strain, M. C.; Farkas, O.; Tomasi, J.; Barone, V.; Cossi, M.; Cammi, R.; Mennucci, B.; Pomelli, C.; Adamo, C.; Clifford, S.; Ochterski, J.; Petersson, G. A.; Ayala, P. Y.; Cui, Q.; Morokuma, K.; Malick, D. K.; Rabuck, A. D.; Raghavachari, K.; Foresman, J. B.; Cioslowski, J.; Ortiz, J. V.; Stefanov, B. B.; Liu, G.; Liashenko, A.; Piskorz, P.; Komaromi, I.; Gomperts, R.; Martin, R. L.; Fox, D. J.; Keith, T.; Al-Laham, M. A.; Peng, C. Y.; Nanayakkara, A.; Gonzalez, C.; Challacombe, M.; Gill, P. M. W.; Johnson, B. G.; Chen, W.; Wong, M. W.; Andres, J. L.; Head-Gordon, M.; Replogle, E. S.; Pople, J. A. *Gaussian 98*, revision A.11.2; Gaussian, Inc.: Pittsburgh, PA, 2001.

(46) Jensen, F. *Introduction to Computational Chemistry*; John Wiley & Sons: New York, 1999.

(47) Helgaker, T.; Jensen, H. J. A.; Jørgensen, P.; Olsen, J.; Ruud, K.; Ågren, H.; Auer, A. A.; Bak, K. L.; Bakken, V.; Christiansen, O.; Coriani, S.; Dahle, P.; Dalskov, E. K.; Enevoldsen, T.; Fernandez, B.; Hättig, C.; Hald, K.; Halkier, A.; Heiberg, H.; Hettema, H.; Jonsson, D.; Kirpekar, S.; Kobayashi, R.; Koch, H.; Mikkelsen, K. V.; Norman, P.; Packer, M. J.; Pedersen, T. B.; Ruden, T. A.; Sanchez, A.; Saue, T.; Sauer, S. P. A.; Schimmelpfennig, B.; Sylvester-Hvid, K. O.; Taylor, P. R.; Vahtras, O. *DALTON*, version 1.2; http://www.kjemi.uio.no/software/dalton/dalton.html: Oslo, Norway, 2001.

(48) *PCMODEL*, version 7.0; Serena Software, Box 3076, Bloomington, IN 47402-3076.